RECENT CUSB RESULTS AND QCD

Juliet Lee-Franzini
SUNY at Stony Brook, Stony Brook, NY, USA

ABSTRACT

The impact of the Upsilon system on QCD, based on CUSB data and analyses, are presented. Results in the area of perturbative QCD include determinations of $\Lambda_{\overline{MS}}$ from $\Upsilon(\Upsilon')\to\gamma gg$ and $\Upsilon(\Upsilon')\to ggg$ and the total widths of the χ_b J=2,1 states. Results in the area of non-perturbative QCD include determinations of the mass and leptonic widths of the higher upsilon resonances (5S and 6S), and the B^*-B mass difference which measures $(Q\bar{q})$ hyperfine splitting. Results from CUSB-II indicate that we have not yet gone beyond QCD in so far as we have not observed any anomalously large Υ radiative decays ($\Upsilon\to\gamma X$).

INTRODUCTION

During the past six years the CUSB[1] Collaboration has mapped a dozen different $(b\bar{b})$ states using the CUSB-I detector (a NaI-Pb glass calorimeter). The masses of these states, as well as the observed major decay modes, are depicted in figure 1. The double lines indicate two pion transitions and single lines indicate photon transitions between the levels, where the solid lines stand for observed transitions and the dashed lines indicate our future goals. While the masses of the Υ's and (center of gravity) of the χ_b's, as well as the B^*-B mass difference, are germaine to testing of non relativistic quark potential models, decay modes of the T's and χ_b's which involve the annihilation of the b and $\bar{b}$ quarks bear on the realm of perturbative QCD and yield determinations of $\Lambda_{\overline{MS}}$.

In the past year we have inferred the existence of the $T(5^3S_1)$ and $\Upsilon(6^3S_1)$ from our data taken during a prolonged scan in the c. of m. energy region between 10.6 and 11.2 GeV, and observed the production of 50 MeV photons (hence of B^*'s) at these resonances. Furthermore we have just finished a test run with a module of the upgraded CUSB detector (a Bismuth Germanate calorimeter: CUSB-II)[2] on the $T(1^3S_1)$, the preliminary results from which give stringent limits on the inclusive branching ratio $T \to \gamma X$ (where X stands for anything) and confirm our previous measurements[3] of the QCD scale parameter $\Lambda_{\overline{MS}}$. These results, and that of an analysis of the χ_b (J=2 and J=1) total widths are discussed in the following.

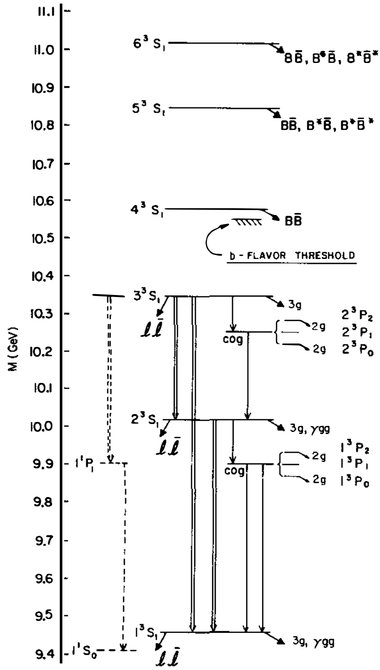

Figure 1 Present Status of T Spectroscopy.

PERTURBATIVE QCD

$\Lambda_{\overline{MS}}$ -- We have measured with CUSB-I the γ spectra of direct photon production from T and T' which are shown in fig. 2 as a function of z ($=E_\gamma/E_{beam}$). We separate high energy γ's from pions statistically by using the difference between the conversion probability of π^0's (i. e. 2γ's) and direct γ's in the first layer of NaI in our detector. The spectra shown in fig. 2 are acceptance corrected and continuum subtracted. Preliminary analysis of our recent data taken with CUSB-II are in good agreement with these spectra. Since within statistics these data are devoid of sharp features, we fit them to a function of the form $z(1-z)^a$ to obtain the total area, thus

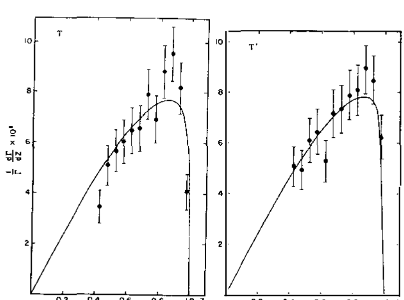

Figure 2 T'(T)→γgg spectra.

obtaining the total production rate of direct photons from T and T'.

Heavy quarkonia are expected to decay mostly via three gluons and a fraction of the time into a photon and two gluons. The ratio of these two partial rates, including next to leading order QCD terms[4], is given by $(36/5)q^2(\alpha/\alpha_s)[1+2.2\alpha_s/\pi]$, where q is the quark charge and α_s is related to the QCD scale parameter $\Lambda_{\overline{MS}}$ including second order corrections[5]. Both the measured rates and the rough shape of the spectra in fig. 2 are consistent with those expected from the Υgg decay mode. We obtain from these measurements:

$\alpha_s(T') = 0.226 \quad +0.067 \ -0.042$,

$\alpha_s(T) \ = 0.197 \quad +0.122 \ -0.054$ and

$\Lambda_{\overline{MS}} = 116 \ +105 \ -57$ MeV from T',

$\Lambda_{\overline{MS}} = \ 80 \ +195 \ -59$ MeV from T data.

These values are in good agreement with those we obtained from measuring $B_{\mu\mu}$ where the theoretical uncertainty is much larger[5].

$\Lambda_{\overline{MS}} = 140 \ +54 \ -24$ MeV from T',

$\Lambda_{\overline{MS}} = \ 95 \ +54 \ -34$ MeV from T data.

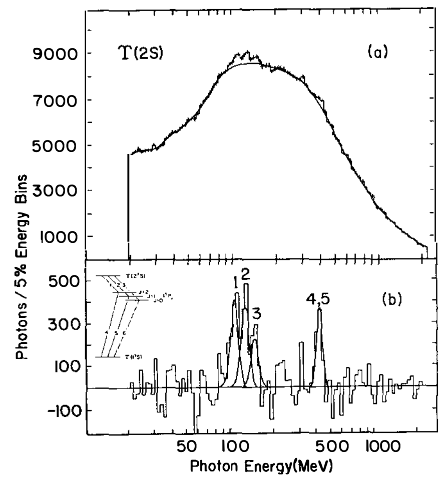

Figure 3 E1 transitions: $T' \to \gamma\chi_b \to \gamma T$

Total Widths of χ_b (J=2,1) states--

Since we observed the (χ_b')'s[7] and the (χ_b)'s[8] the understanding of relativistic corrections to photon transition rates has greatly improved[9]. Whenever the initial and final states have differing number of nodes in their radial wave functions, for ex. $T'' \to \gamma + 1^3P_J$, the rates are most sensitive to such corrections and are very model dependent. CUSB's small upper limit for this transition not only favors the choice of the potentials of reference 9, but also indicates that relativistic corrections are likely to be small in the $b\bar{b}$ system. Calculations of the E1 rate for transitions such as $1^3P_J \to \gamma + T$ are particularly reliable. These we make use of to estimate the total widths of the χ_b states which are expected to be very narrow hence not directly measurable.

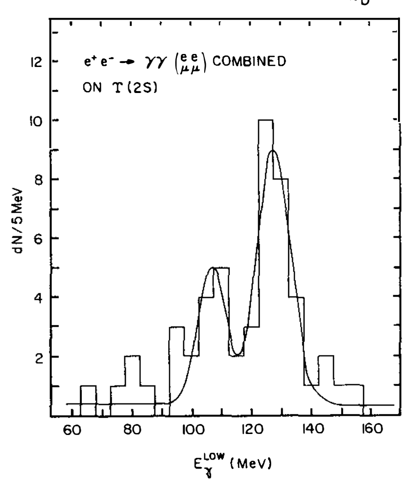

Figure 4 Projection of exclusive cascade γ's on low E_γ axis.

We show in fig. 3 the photon lines to and from the χ_b observed in the CUSB-I inclusive photon spectrum. The line labelled 4,5 is identified as the E1 transitions from the χ_b J=2 and J=1 states to the T (transtions from the J=0 state is expected to be small). We obtained the branching ratio BR from $T'\to\chi_b$ J=2,1)γ (lines 1+2) to be (6.1±1.4)% and (5.9±11.4)% respectively and the product BR of $T'\to\chi_b(J=2,1)\gamma\to T\gamma$ to be (4±1)%. In fig. 4 we show the energy distribution of the lower energy photon from events of the type $T'\to\gamma\chi_b\to\gamma T$ where the T decays into an e^+e^- or a $\mu^+\mu^-$ pair. The 107 MeV line is associated with the $T'\to\chi_b(J=2)$ transition and the 128 MeV line with the $T'\to\chi_b(J=1)$ transition. Note that their intensities are in the ratio of (0.51±0.25):1. We deduce that the E1 BR of $\chi_b(J=2)$ to T is (20±5)% and the E1 BR of $\chi_b(J=1)$ is (47±18)%. These values are in excellent agreement with potential model calculations and we use these BR's and the computed E1 rates to obtain

$\Gamma_{tot}(1^3P_2(b\bar{b})) = (173\pm43\pm18)$ keV, $\Gamma_{tot}(1^3P_1(b\bar{b})) = (67\pm26\pm10)$ keV.

The first error is due to the error in measuring the BR's and the second to an estimate of the uncertainty in the calculated E1 rates. QCD calculations[10] give $(\chi_b(J=2)\to gg)\approx190$ keV and $\Gamma(\chi_b(J=2)\to q\bar{q}g)\approx60$ keV with uncertainties on the order of 50%. The excellent agreement between the two sets of rates indicate that we may use the χ_b widths someday to obtain an independent measurement of α_s.

NON PERTURBATIVE QCD

Higher T resonances --

Fig. 5 shows the CUSB scan at CESR above the T(4S) region[11]. Fig. 5a shows $R_{visible}$ for all hadronic events, the bottom figure is R_{vis} for events which passed a thrust cut, note the suppressed zero in both figures. Both show complicated structures, which survive the thrust cut ($B\bar{B}$ events are less "thrusty" than continuum events) and therefore are resonance associated. The tall peak on the left of the figures is the T(4S), which lies below the B^* production

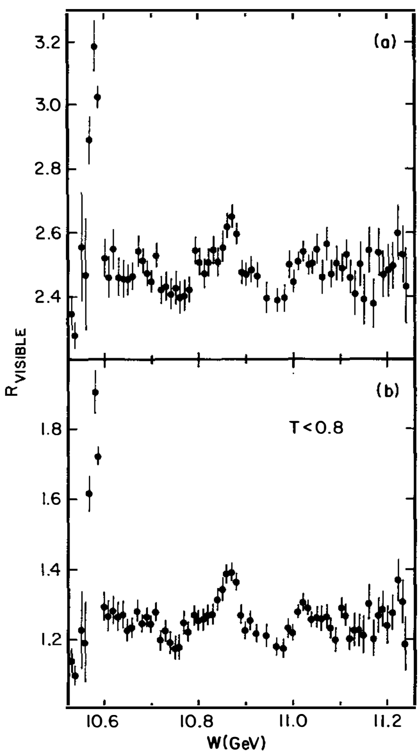

Figure 5 $R_{visible}$ vs E_{cm} .

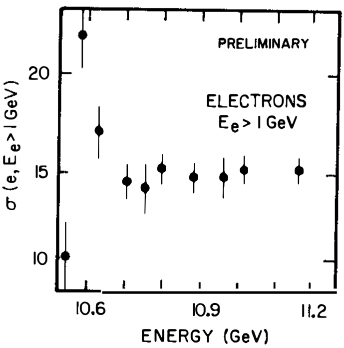

Figure 6 $\sigma(e,E_e>1$ GeV) vs E_{cm}

threshold[12]. Another evidence of $b\bar{b}$ production at these energies is the increase in production of high energy electrons (E>1 GeV, hence from β-decay of b-quarks) as shown in figure 6.

Since the mass difference between B and B^* is ≈50 MeV and the mass difference between the strange and normal B's is ≈100 MeV, six thresholds $B_{d(u)}\bar{B}_{d(u)}$, $B_{d(u)}\bar{B}^*_{d(u)}$, $B^*_{d(u)}\bar{B}^*_{d(u)}$, $B_s\bar{B}_s$, $B^*_s\bar{B}_s$, $B^*_s\bar{B}^*_s$, occur within the E_{cm} range of 10.55 and 10.85 GeV indicated by arrows at the bottom of fig. 7b. Furthermore, all potential models indicate that three higher T resonances, T(4S), T(5S) and T(6S) are expected to be present in the E_{cm} range 10.5 to 11.5 GeV. We performed a coupled channel calculation using the Eichten et al[13] potential model, assuming only four T(nS) states and the six thresholds. In figure 7 the CUSB computed curve is shown superimposed over our data, the agreement between them is remarkable, especially considering the simplifying assumptions made. In fig. 7a the separate contribution from each T resonance is shown. In fig. 7b the separate contributions from ordinary and strange B mesons are shown. One notes from these figures that the dominant contribution to the cross section is due to the T(5S) and that it couples to all six two body channels. The position of this resonance agrees with most potential model

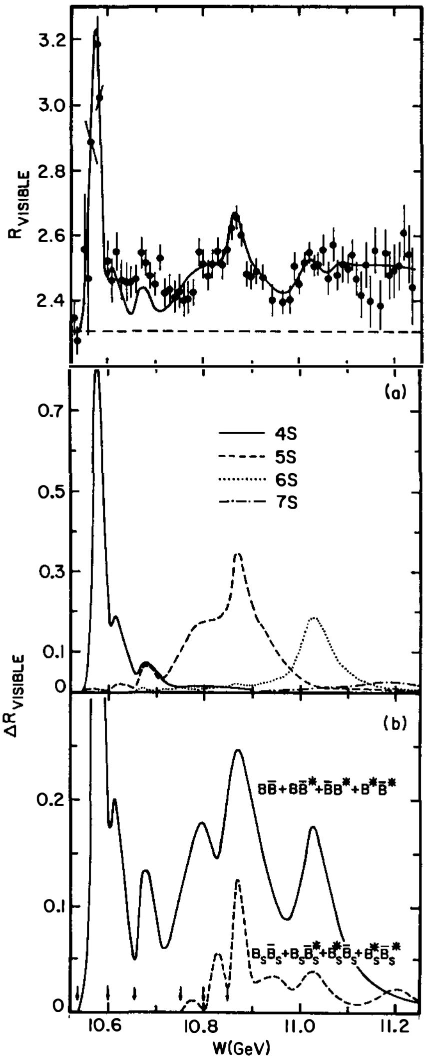

Figure 7 CUSB Model Calculation: top, superimposed over data, 7a, contributions from T(nS), 7b, from B's and B_s's.

calculations once the proximity to many open channels is taken into account, an example being the Tornquivst calculation[14]. Similarly, most of the cross section excess around 10.6 GeV is due to Υ(4S) coupling into B^*B and B^*B^* channels. There is room for some expected D state contribution, but in my opinion does not call for the postulation of any exotic new states. The identification of the sharp rise of the cross section at 11 GeV with the presence of the Υ(6S) state is consistent, if not overwhelmingly compelling, with the data and the model calculation. The resonance parameters are tabulated below.

Resonance	Mass (GeV)	Γ (MeV))	Γ_{ee}(keV)
Υ(4S)	10.5774±0.001	25±2.5	0.283±0.037
Υ(5S)	10.845 ±0.020	110±15	0.365±0.070
Υ(6S)	11.02 +0.03	90±20	0.156±0.040

In conclusion the behavior of $(b\bar{b})$ states above the free flavor threshold is well described by nonrelativistic potential models (with coupled channel modifications). Our model calculation also predicts that B^*'s should be produced above 10.6 GeV. In figure 8 we show the energy dependence of the $B\bar{B}$,$B^*\bar{B}+B\bar{B}^*$, and $B^*\bar{B}^*$ cross section (where B stands for either ordinary or strange B mesons). In short, in the energy region between 10.6 to 11.1 GeV we expect ≈1.4 B^* per $(b\bar{b})$ event.

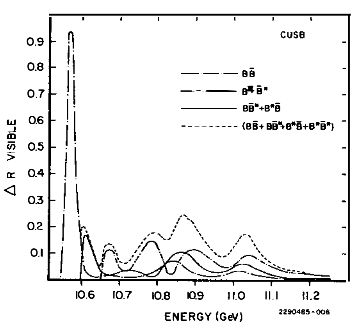

Figure 8 $\Delta R_{visible}$ vs E_{cm} for $B\bar{B}$, $B\bar{B}^*+\bar{B}B^*$, $B^*\bar{B}^*$.

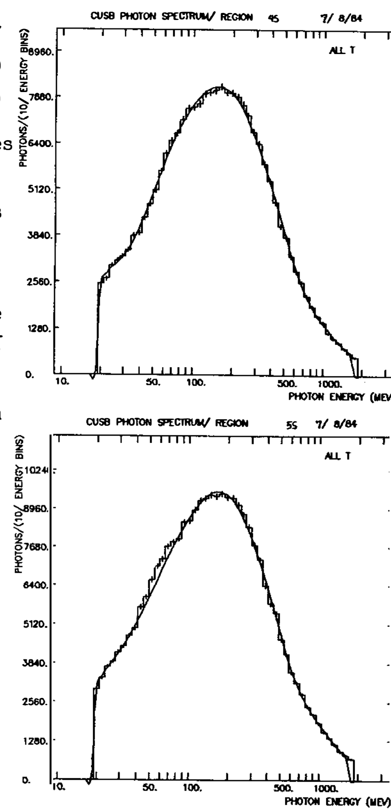

Figure 9 Inclusive Υ spectra: top, Υ(4S), bottom, Υ(5S)

Observation of B^* --

It has been known for some time now that B^*'s (vector B mesons) are not produced on the Υ(4S) where $B\bar{B}$'s are produced copiously[12]. The method of search is founded upon the fact that since the B^*-B mass difference is known from scaling arguments to be ≈50 MeV, the only decay mode available to the B^* is the return to the ground state via emission of a photon. The search for such photons yielded 90% c. l. limits of the order of (6-9)% B^* per $(b\bar{b})$ events. The inclusive photon spectrum is shown at the top of figure 9, it shows no excess of ≈50 MeV photons. This result is fully consistent with our model calculation, see also fig. 8. The photon spectrum on the Υ(5S) is shown at the bottom of fig. 9, together with the polynomial fit to the Υ(4S) spectrum. An apparent excess is visible; a simple subtraction yields a signal in excess of seven sigmas whose width agrees with our computed resolution (including Doppler broadening), centered at ≈50 MeV. Recall that the fraction of events which contain a b quark pair in the energy range above the Υ(4S) is ≈7% and that the B^*'s have ≈15% Doppler widths, both factors render the photon search difficult. We enhanced the $(b\bar{b})$ fraction by (i) applying a thrust cut, choosing more spherical events, see fig. 10b, (ii) applying E_{cm} cut, choosing regions where Υ resonances are known to exist, see fig. 10c. We fit a cubic plus a gaussian of known width to obtain the signals shown in figure 10.

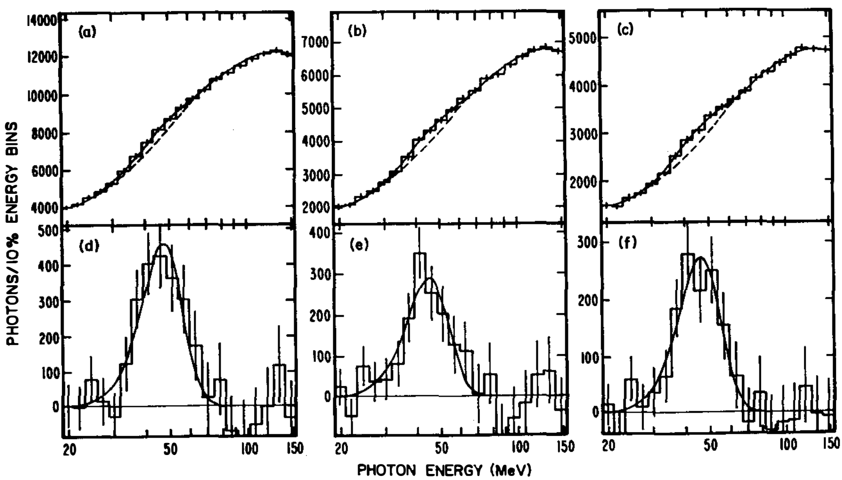

Figure 10 Photon spectra for events without an observed lepton. a) $10.62<E_{cm}<11$ GeV, b) same E_{cm} as a, thrust <0.83, c) E_{cm} 10.62-10.72, 10.78-10.9, 11-11.12 . d) background subtracted γ signal, $N_\gamma=2112\pm424$, corrected $E_\gamma= 51.6\pm1.7$ MeV, e) region b subtracted γ signal, $N_\gamma=1405\pm350$, corrected $E_\gamma=49.1\pm2.0$ MeV and f) region c subtracted γ signal, $N_\gamma=1286\pm272$, corrected $E_\gamma=50.5\pm1.8$ MeV.

An alternate way to enhance the fraction of $(b\bar{b})$ events is to require the presence of a high energy lepton (e or μ with energy > 1GeV). In figure 11 we show the γ spectrum of such lepton tagged events (solid line) superimposed over a background curve (dotted curve) constructed with the proper fractions of $(b\bar{b})$

events from the $\Upsilon(4S)$ and continuum events. While the lepton tagging requirement reduces the event sample tenfold, the signal/background ratio is enhanced by a factor of four. The subtracted photon signal shown in fig. 11 contains 123±28 photons in the region 35-65 MeV. We thus have a five sigma effect from the restricted (no lepton) inclusive spectrum and a 4.4 sigma effect from the lepton tagged events. The number of $B^*/(b\bar{b})$ event is 1.4±0.5 from the former sample and 1.5±0.5 from the latter. Note that both are in good agreement with our model calculation. The mass difference $M(B^*)-M(B)$ we obtain is 52 ± 2 ± 4 MeV [15].

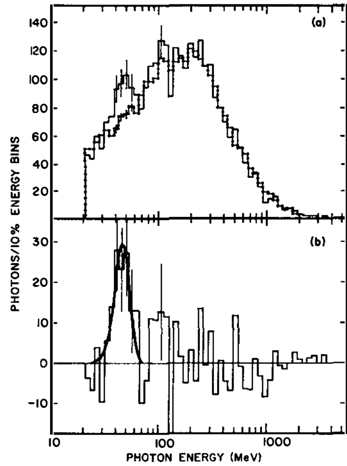

Fig. 11 Lepton Tagged Υ spectrum

Our mass difference between the vector and pseudoscalar B mesons is in good agreement with many potential model calculations[16]. In the naive nonrelativistic picture, this hyperfine splitting due to one gluon exchange is given by[17] $\{M(Q\bar{q})^*-M(Q\bar{q})\}=(32\pi\alpha_s/9M_Q m_q)|\Psi(0)|^2$, $\{M^2(Q\bar{q})^*-M^2(Q\bar{q})\}=(64\pi/9)\times\{\alpha_s|\Psi(0)|/m_q\}$. The CUSB ΔM^2 is 0.551 ± 0.043 GeV^2. This value joins a long list of such mass square differences ($\rho-\pi$, K^*-K, D^*-D, F^*-F) which are all equal $\approx 0.57\pm0.02$ GeV^2. This implies that $\{\alpha_s|\Psi(0)|^2/m_q\}$ is a constant for all heavy-light ($Q\bar{q}$) mesons.

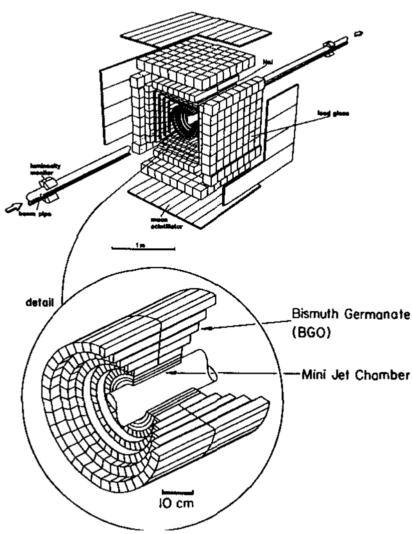

Figure 12 CUSB-II Detector

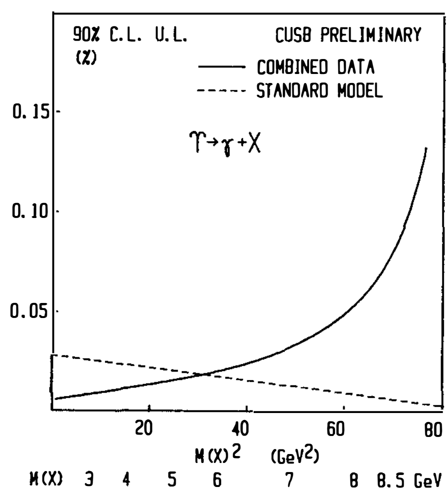

Figure 13 Preliminary CUSB-II $\Upsilon\to\gamma X$ Limit

BEYOND QCD?

The CUSB detector is undergoing an upgrade by inserting within the NaI array, a twelve radiation length cylinder of Bismuth Germanate (CUSB-II, see figure 12). During last fall we ran on the Υ(1S) with a reduced (9 radiation lengths instead of 12) quadrant of the BGO cylinder in place, such that it subtended 1/4 of the solid angle while the rest is covered by sodium iodide. Approximately a total of 400,000 Υ's were produced during the 22 pb^{-1} run. The inclusive photon spectra in NaI and in BGO were examined, no monochromatic signal consistent with our known resolutions was found. In figure 13 we show our preliminary limit for $\Upsilon \to \gamma X$, where X stands for anything. The dashed line is the predicted branching ratio for $\Upsilon \to \gamma H$ via the Wilczek[18] mechanism for a Higgs boson of the standard model. Our limit is preliminary because intensive Monte Carlo studies are underway to determine our efficiency as a function of assumed X decay modes. However, it is clear that we have not gone "Beyond QCD" yet, since we have not seen any anomlously high rate of $\Upsilon \to \gamma X$ production.

ACKNOWLEDGEMENTS

The author acknowledges all her CUSB-I and CUSB-II colleagues, but especially R. D. Schamberger for innumerable conferrings during and after data analyzes. The author's research is supported in part by the U. S. National Science Foundation.

REFERENCES

1. CUSB-I members include: P. Franzini, D.Son, P.M. Tuts, S. Youssef and T. Zhao of Columbia University; J. Lee-Franzini, J.E. Horstkotte, C. Klopfenstein, D.M.J. Lovelock, L. Romero, and R.D. Schamberger of Stony Brook; K. Han, R. Imlay, W. Metcalf and V.Sreeedhar of Louisiana S.U.; H. Dietl, G. Eigen, V. Fonseca, E. Lorenz and G. Mageras of Munich, M.P.I.
2. CUSB-II members include: P. Franzini, D. Son, P.M. Tuts, S. Youssef and T. Zhao of Columbia University and J. Lee-Franzini, T.M. Kaarsbrg, C. Klopfenstein, D.M.J. Lovelock, S. Sontz, R.D. Schamberger, J. Willins, C. Yanagisawa and S. Yoakum of SUNY at Stony Brook.
3. R. D. Schamberger et al., Phys. Lett.138B (1984) 225.
4. S. Brodsky, G.P. Lepage and P.B. Mackenzie, Phys. Rev. D28 (1983) 228.
5. A. J. Buras et al., Rev. Mod. Phys. 52 (1980) 199.
6. P. B. Mackenzie and G. P. Lepage, Phys. Rev. 47 (1981) 1244.
7. K. Han et al., Phys. Rev. Lett. 49 (1982) 1612.
   G. Eigen et al., Phys. Rev. Lett. 49 (1982) 1616.
8. C. Klopfenstein et al., Phys. Rev. Lett. 51 (1983) 160,
   F. Pauss et al., Phys. Lett. 130B (1983) 439.

9. P. Moxhay and J. L. Rosner, Phys. Rev. D28 (1983) 1132.
   R. McClary and N. Byers, Phys. Rev. D28 (1983) 1692.
10. R. Barbieri, R. Gatto and R. Kogerler, Phys. Lett. 60B (1976) 183,
    R. Barbieri, R. Gatto and E. Remiddi, Phys. Lett. 61B (1976) 465.
11. D. M. J. Lovelock et al., Phys. Rev. Lett. 54 (1985) 377.
12. R. D. Schamberger et al., Phys. Rev. D26 (1982) 720; D30 (1984) 1985.
13. E. Eichten, Phys. Rev. D22 (1980) 1819.
14. N. A. Tornqvist, Phys. Rev. Lett. 53 (1984) 878.
15. J. Lee-Franzini, in Proceedings of the 22nd International Conference on High Energy Physics, edited by A. Meyer and E. Wieczorek (Karl Marx Univ., DDR, 1985) 189; K. Han et al, sub. to Phys. Rev. Lett.
16. E. Eichten et al., Phys. Rev. D21 (1980) 203;
    A. Martin, Phys. Lett. 103B (1981) 51.
17. J. M. Richard, review talk at January workshop.
18. F. Wilczek, Phys. Rev. Lett. 40 (1978) 220.